Mechanisms Involved in the Formation of Biocompatible Lipid Polymeric Hollow Patchy Particles

Nashaat Rasheed,[†,‡] Ali A. Khorasani,[‡,§] Juan Cebral,[†,‡] Fernando Mut,[†] Rainald Löhner,[||] and Carolina Salvador-Morales*[,†,‡]

[†]Bioengineering Department, [‡]Krasnow Institute for Advanced Study, [§]Department of Chemistry and Biochemistry, and [||]Center for Computational Fluid Dynamics, College of Sciences, George Mason University, Fairfax, Virginia 22030, United States

S *Supporting Information*

ABSTRACT: Patchy polymeric particles have anisotropic surface domains that can be remarkably useful in diverse medical and industrial fields because of their ability to simultaneously present two different surface chemistries on the same construct. In this article, we report the mechanisms involved in the formation of novel lipid−polymeric hollow patchy particles during their synthesis. By cross-sectioning the patchy particles, we found that a phase segregation phenomenon occurs between the core, shell, and patch. Importantly, we found that the shear stress that the polymer blend undergoes during the particle synthesis is the most important parameter for the formation of these patchy particles. In addition, we found that the interplay of solvent−solvent, polymer−solvent, and polymer−polymer−solvent interactions generates particles with different surface morphologies. Understanding the mechanisms involved in the formation of patchy particles allows us to have a better control on their physicochemical properties. Therefore, these fundamental studies are critical to achieve batch control and scalability, which are essential aspects that must be addressed in any type of particle synthesis to be safely used in medicine.
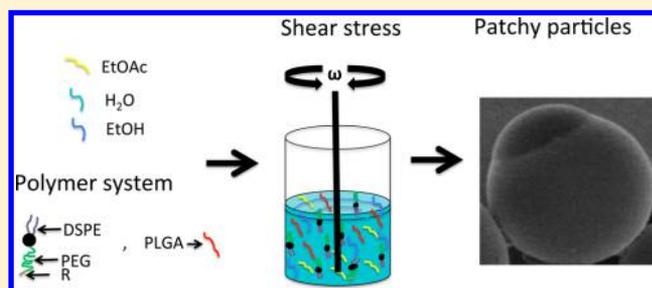
1. INTRODUCTION

Patchy particles are a class of anisotropic particle that are characterized by their one or more surface-exposed domains with different surface chemistry relative to the rest of the particle.[1] Over the past 6 years, there have been significant theoretical and experimental developments in the study of patchy particles.[2−12] These extensive research efforts are fueled by the hope of exploiting the unique organic or inorganic anisotropic segregated surface domains that can exist on organic particles for anisotropic site-specific modifications.[13−15] This anisotropic feature is greatly advantageous in several fields, including drug delivery, diagnostics, sensors, and photonics, because it allows us to expand, improve, and complement the functions and designs of the materials used in these areas. For example, anisotropic particles may enable the (a) formation of building blocks that can eventually form supraparticular assemblies,[16,17] (b) development of well-defined discrete multimodality platforms for drug delivery,[18−20] imaging,[19−21] and diagnostic purposes,[22] and (c) synthesis of multihybrid materials.[18,23]

Today, patchy particles can be synthesized via at least six different techniques: template-assisted fabrication,[15,17,24] evaporation-driven colloidal assembly,[17,25,26] particle lithography,[17,27,28] glancing-angle vapor deposition,[17,29,30] electrified jetting,[17,19,20] and phase segregation.[31−33] The most recent and notable examples of phase-segregated patchy particles include lipid−polymeric patchy particles,[31] ice cream cone particles,[32]

and golf ball particles.[33] Our patchy particles fall in the first category. Currently, there is considerable information on the thermodynamics that cause phase segregation in different polymer blends;[34−36] however, there are no published papers that report the thermodynamics involved in the phase segregation of the poly(D,L-lactide-*co*-glycolide) (PLGA)−lipid-PEGylated-functional groups (LPFGs) system. Two years ago, we discovered and published a new class of patchy particle with a core−shell structure.[31] This particle is formed from two elements: (1) hydrophobic polymers, such as PLGA, which form the hydrophobic core that encapsulates a payload, and (2) 1,2-distearoyl-*sn*-glycerol-3-phosphoethanolamine (DSPE)-*N*-poly(ethylene glycol) (PEG) with amino, methoxyl, or maleimide terminal groups (DSPE-PEG-NH$_2$, DSPE-PEG-OCH$_3$, and DSPE-PEG-MAL), which form one or two patches on the particle's core. The formation of such patches resembles the phase segregation phenomenon observed in many polymer blends[37−39] and lipids rafts.[40] However, since our polymer blend system is quite complex because it involves two different polymers (i.e., PLGA and LPFGs) and a trisolvent composition (i.e., water, ethanol, and ethyl acetate), it is likely that the formation of patchy polymeric particles is due to an interplay of thermodynamic, chemical, and physical factors. Here, we report the mechanisms involved in the formation of these lipid−

polymeric patchy particles. In particular, we investigated in detail the solvent—solvent, polymer—polymer, and polymer—polymer—solvent interactions that take place in each step of the particle's synthesis. Therefore, this research contributes to the polymer thermodynamics field by generating the first thermodynamic analysis on this particular polymer—lipid—polymer system.

2. MATERIALS AND METHODS

Materials. Solvents were purchased at analytical grade from Sigma-Aldrich (St. Louis, MO). DSPE and PEG-based polymers purchased from Avanti Polar Lipids (Alabaster, AL) and Laysan Bio (Arab, AL). PLGA was purchased from Lactel (Pelham, AL). Fluorescent dyes, reactive probes, and biological reagents were purchased from Life Technologies (USA).

Particle Synthesis and Characterization. Particles were prepared by a single-emulsion method. The aqueous phase of the mixture was prepared by dissolving LPFGs, labeled or unlabeled, to a concentration of 1 mg/mL in 4% ethanol. To this solution 6 mL of 4% ethanol was added, and the solution was homogenized at 1000 rpm for 15 s. 4 mL of PLGA solution (15 mg/mL in ethyl acetate) was immediately added to the aqueous phase. The mixture was homogenized at 4000 rpm for 1 min using a L5M-A high shear mixer and 5/8 in. tubular mixing assembly. 50 mL of deionized water was added dropwise to the emulsified mixture, and the volatile solvent was allowed to evaporate overnight. Particles were centrifuged at 2000 rpm, using Millipore Amicon Ultra centrifugal filter units with a MWCO of 100 kDa. Particles were examined with a FE-SEM (Zeiss) operating at 1.00 kV accelerating voltage.

Focused Ion Beam Cross Sections. Patchy microparticles were cross-sectioned using a FEI FIB with a gallium ion source operated at 1 kV, SE mode, and 25000× magnification. Patchy microparticles were previously coated with gold—palladium alloy to protect particles from the ion beam.

Studies on Surface Tension While Varying the LPFGs' Concentration. The surface tension of LPFGs while varying their concentration was taken with a Ramé-Hart tensiometer—goniometer, using the pendant drop method. LPFGs solutions were considered the droplet phase, and air was taken as a reference. 15 mg of DSPE-PEG (2000)-NH$_2$ was dissolved in 5 mL of 4% (v/v) ethanol to a concentration of 3.0 mg/mL. This concentration was subsequently diluted to prepare the other concentrations. A 5 μL drop was suspended from a syringe needle, and the ST was measured. Each measurement was taken in triplicate.

Interfacial Surface Tension Studies Varying the Ethanol Concentration. The interfacial surface tension between the aqueous and organic phases was measured with a Ramé-Hart tensiometer—goniometer using an inverted pendant drop method. PLGA solution was considered the organic drop phase while ethanol or ethanol/LPFGs solution was taken as a reference in the aqueous phase. 75:25 PLGA (IV of 0.55—0.75 dL/g in CHCl$_3$) was dissolved in ethyl acetate to a concentration of 15 mg/mL for the droplet phase. Ethanol—water mixtures were prepared by volume percent. For ethanol/LPFGs reservoirs, 20 mg of DSPE-PEG-NH$_2$ was dissolved in 200 mL of ultrapure water to a concentration of 1 mg/mL. 20 mL solutions of each ethanol concentration were prepared by adding 5 mL of 1 mg/mL LPFGs solution to a vial. To this vial, additional water and ethanol were added to reach the desired percent ethanol (for 2% ethanol, 400 μL of ethanol and 14.6 mL of deionized water were added). Additional water and ethanol were added to this solution to obtain a LPFGs concentration of 0.25 mg/mL and the desired percent ethanol by volume.

Colorimetric Method. For each 1 mg of DSPE-PEG-NH$_2$ in solution, 10 μg of Alexa-633 carboxylic acid succinimidyl ester was dissolved in N,N-dimethylformamide and allowed to react with the LPFGs for 1 h. The resulting solution was transferred to Spectra/Por dialysis tubing with a MWCO of 2000 Da and dialyzed in deionized water overnight at 4 °C. PLGA of the desired viscosity was dissolved at a concentration of 15 mg/mL in ethyl acetate. 2 mL of the lipid

solution were added to a beaker or vial, and an additional 6 mL of 4% ethanol was added for a pre-emulsification step. Then, 4 mL of the PLGA solution was added to above the aqueous phase. Samples in vials were shaken vigorously for 30 s by hand, and samples in beakers were homogenized at 4000 rpm for 1 min and then transferred to glass scintillation vials. The phases were allowed to separate for 1 h, and then the phases were syringed off into separate open vials and allowed to evaporate overnight, recording the initial volume. Evaporated samples were then reconstituted to their initial volume with 4% ethanol, and any PLGA residue was filtered using Millipore Amicon Ultra Centrifugal Filter Units with a MWCO of 100 kDa. The fluorescence of the Alexa Fluor 633 was read with an excitation wavelength of 600 nm and an emission wavelength of 640 nm using a Biotek Synergy 2 plate reader. A calibration curve for the system was prepared by conducting serial dilutions of the labeled 0.25 mg/mL DSPE-PEG-NH$_2$-A633 solution in 4% ethanol. The percentage of unreactive LPFGs was determined based on the difference between the initial mass of LPFGs used in the synthesis and the mass of detected fluorescent LPFGs divided by the initial mass of LPFGs multiplied by 100% (i.e., $[(m_{initial} - m_{detected})/m_{initial}] \times 100\%$). The same rationale was used to determine the percentage of LPFGs that interacted with PLGA.

Differential Scanning Calorimetry Measurements. Thermal analyses of the materials were run on a TA Instruments T100 differential scanning calorimeter from −90 to 90 °C, at a rate of 10 °C/min. Samples were lyophilized prior to thermal scans. Enthalpies of transition were calculated by normalizing the transition peak of the thermogram and integrating with Origin software.

Transmission Electron Microscopy Studies To Determine the Critical Micelle Concentration of DSPE-PEG-NH$_2$ and DSPE-PEGm. A 5 mg/mL stock solution of DSPE-PEG-NH$_2$ (Avanti Polar lipids) in 4% ethanol was diluted to a concentration of 1×10^{-3} M, and serial dilutions were made to prepare LPFGs at 0.00084, 0.0028, and 0.028 mg/mL concentrations. From these concentrations, TEM samples were prepared by pipetting 10 μL of LPFGs solutions onto TEM sample copper grids. Samples were then stained with 10 μL of uranyl acetate (2% v/v), tapped to remove excess stain solution, and allowed to dry overnight. One sample was prepared with DSPE-PEGm at a concentration of 1×10^{-3} M, loaded in a copper grid, stained with uranyl acetate, and analyzed with TEM. In addition, we prepared three more samples to be analyzed with TEM. The first solution was prepared only with LPFGs at a concentration of 1 mg/mL in 4% ethanol. The second solution contained 2 mL of LPFGs (1 mg/mL) in 4% ethanol and 6 mL of 4% ethanol. Therefore, the final concentration of LPFGs after adding 6 mL of 4% ethanol is 0.25 mg/mL. The third solution was prepared with 2 mg of LPFGs (1 mg/mL) dispersed in 4% ethanol, 6 mL of 4% ethanol, and mixed with PLGA (60 mg) dissolved in 4 mL ethyl acetate. After adding PLGA dissolved in ethyl acetate, the final concentration of LPFGs in this solution is 0.16 mg/mL. The samples were analyzed with TEM. 10 μL of each prepared sample was placed on a copper grid. Subsequently, 10 μL of uranyl acetate (2% v/v) was added to the copper grid. All the samples mentioned were examined a TecnaiG^2 Spirit BioTWIN transmission electron microscope at 80 kV, and images were recorded with an AMT 2k CCD camera.

Scanning Electron Microscopy Studies. Microparticles were placed after the emulsification, during and after the evaporation step on a silicon wafer and mounted on a stub to be analyzed with FE-SEM (Zeiss). The FE-SEM was operated at 1 kV accelerating voltage and using a secondary electron detector.

Computational Fluid Dynamics. In order to demonstrate the dependence of the fluid shear stress on the size of the gap between the inner diameter of the homogenizer tubular assembly's workhead and the rotor shaft, computational fluid dynamics (CFD) simulations were carried out for varying gap sizes. The numerical solutions of 3D incompressible Navier—Stokes equations were obtained with an edge-based finite element solver developed in-house. Unstructured grids composed of tetrahedral elements were generated and locally refined near the inner wall to obtain at least two points within the gap. The resulting mesh had approximately 3 million elements. We modeled the

rotating piece using immersed boundary methods based on unstructured grids. The rotor shaft was set in rigid-body rotation around its axis at 4000 rpm. No slip boundary conditions were applied at all body surfaces, including the rotating rotor shaft. The polymer fluid density was set to 1.0 g/cm^3 and the viscosity to 0.031 dyn s/cm^2. The viscosity of the polymer solution was measured using a MCR702 rheometer (Anton Paar GmbH) with a double-gap configuration. We used an explicit three-stage Runge–Kutta scheme with CFL = 0.6 and a maximum time step of 5×10^{-5} to advance the flow solution. All simulations were carried out in parallel on shared memory computers using OpenMP and were run on 16 processors. We saved results at 1.5 $\times 10^{-4}$ s intervals and created animations of the wall shear stress in the gap region.

3. RESULTS AND DISCUSSION

To investigate to what extent the phase segregation phenomenon was involved in the patchy particle's formation, the focused ion beam (FIB) technique was used to cross section a patchy particle as shown in Figure 1B. The cross
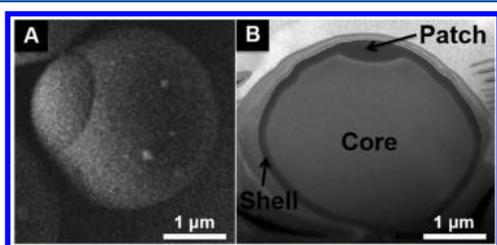
Figure 1. External and internal morphology of a patchy particle. (A) SEM image of particle with a core–shell–patch structure. (B) FIB cross section of the patchy particle exhibiting a patch–shell–core morphology. The outermost layer of the cross section is a metal coating layer to prevent damage of the particle by the FIB. (See Supporting Information for a movie of the cross section of patchy particles.)

sections exhibit two different contrasts, which suggest the segregation of PLGA and LPFGs. The LPFGs show higher contrast than PLGA. The observed indentation in the internal interface of the core–shell does not explicitly reveal the origin of the phase segregation of the polymers. Thus, the cross section studies led us to believe that other factors may be involved in the formation of the patch including the interplay of chemical (solvent–solvent, polymer–polymer, and polymer–polymer–solvent interactions) and physical (shear stress) factors.

Solvent–Solvent Interaction. Our initial step to further understand the polymer phase segregation phenomenon observed in our patchy particles was to study the solvent–solvent interaction. Three solvents were used in the synthesis of these patchy particles: ethyl acetate, ethanol, and water. Each solvent has a certain degree of miscibility with each other, as shown in a ternary phase diagram for this solvent system.[41] The interaction between these solvents can be summarized using Hansen solubility parameters, using the principle of "like dissolves like."[42] Although all three solvents have similar dispersion forces, differences in their polarity and hydrogen bonding make them immiscible between each other to a certain extent. Water is the most polar with the greatest degree of hydrogen bonding; ethyl acetate is the least polar of the solvents, with less hydrogen bonding; and ethanol has values intermediate to the other two solvents. Nevertheless, it is well-known that ethyl acetate and water are miscible to a concentration of 8.3 g/100 mL (8.3 mass %). Because this

miscibility is not insignificant, it might play an important role in the solvent–solvent interaction. In our synthesis, the ratio of the organic to aqueous phase is 1:2. The aqueous phase is composed of 4% ethanol, which ultimately contributes 2.67% of the total solvent volume used in the emulsification step. At this solvent composition, very distinct phases are formed after mixing the solvents. To further investigate the role of solvent–solvent interaction in the formation of patchy particles, we investigated the interaction between LPFGs and 4% ethanol by conducting surface tension (ST) and transmission electron microscopy (TEM) studies. By conducting this type of study, we wanted to know if lipid-based structures were formed during the pre-emulsification step.

Polymer–Solvent Interaction. To determine if a lipid-based structure was formed during the pre-emulsification step, we investigated if there were changes in the surface tension of the LPFGs' solution due to their concentration. Indeed, we found that there were two abrupt changes in the ST of the LPFGs prepared at different concentrations as shown by the graph in Figure 2. These abrupt changes in the ST could indicate the formation of different lipid-based structures (e.g., liposomes, bilayers, or micelles). TEM studies corroborated the formation of lipid-based structures with distinctive morphologies at different concentrations of LPFGs (Figure 2A–F). Two prominent abrupt changes in ST are observed at 0.0028 and 0.25 mg/mL. At 0.0028 mg/mL, flower-like structures are formed (Figure 2B). It is not surprising that these structures are formed at this concentration because the critical micelle concentration of DSPE-PEGm is approximately 0.00281 mg/mL, as reported in the literature[43] and observed with TEM (Figure 2, right side). At this concentration of DSPE-PEGm, micelles are formed. Although round micelles are not formed with 0.0028 mg/mL of DSPE-PEG-NH$_2$, it is clear that the critical micelle concentration (CMC) of DSPE-PEG-NH$_2$ is close to that concentration. At or above CMC, we would expect to see well-formed spherical phase boundaries between the micelles and the surrounding solution. According to the TEM studies, complex structures such as rod-shaped micelles can be formed above the CMC of DSPE-PEG-NH$_2$ (Figure 2C). Below this concentration, DSPE-PEG-NH$_2$ begins to form lipid-based structures, but these structures are not fully formed, giving rise to nonspherical arrangement of lipids, as shown in Figure 2A,B.

We also observed the formation of a lipid-based structure at the concentration used for the synthesis of patchy particles (1 mg/mL) (Figure 2D). TEM studies of LPFGs dispersed in 4% ethanol and subsequently mixed with PLGA dissolved in ethyl acetate indicate the formation of liposomes (Figure 2D–F). We found that the physical integrity of these liposomes relies on the interaction between LPFGs and the solvent system. For example, well-structured liposomes are formed at the concentration of 1 mg/mL of LPFGs in 4% ethanol (Figure 2D). We observed that the physical integrity of liposomes is compromised when an extra 6 mL of 4% EtOH was added to 2 mL of LPFGs (1 mg/mL) (Figure 2E). This phenomenon might be due to the fact that the interaction between the PEG-NH$_2$ fragment of the LPFGs and the additional molecules of 4% ethanol is greater than the interaction among the LPFGs molecules that already formed liposomes. The additional 4% ethanol molecules incorporated in the solvent system attract or disperse the PEG-NH$_2$ fragment of LPFGs causing the disruption of liposomes. The incorporation of PLGA dissolved in ethyl acetate enhances the disruption of these liposomes as
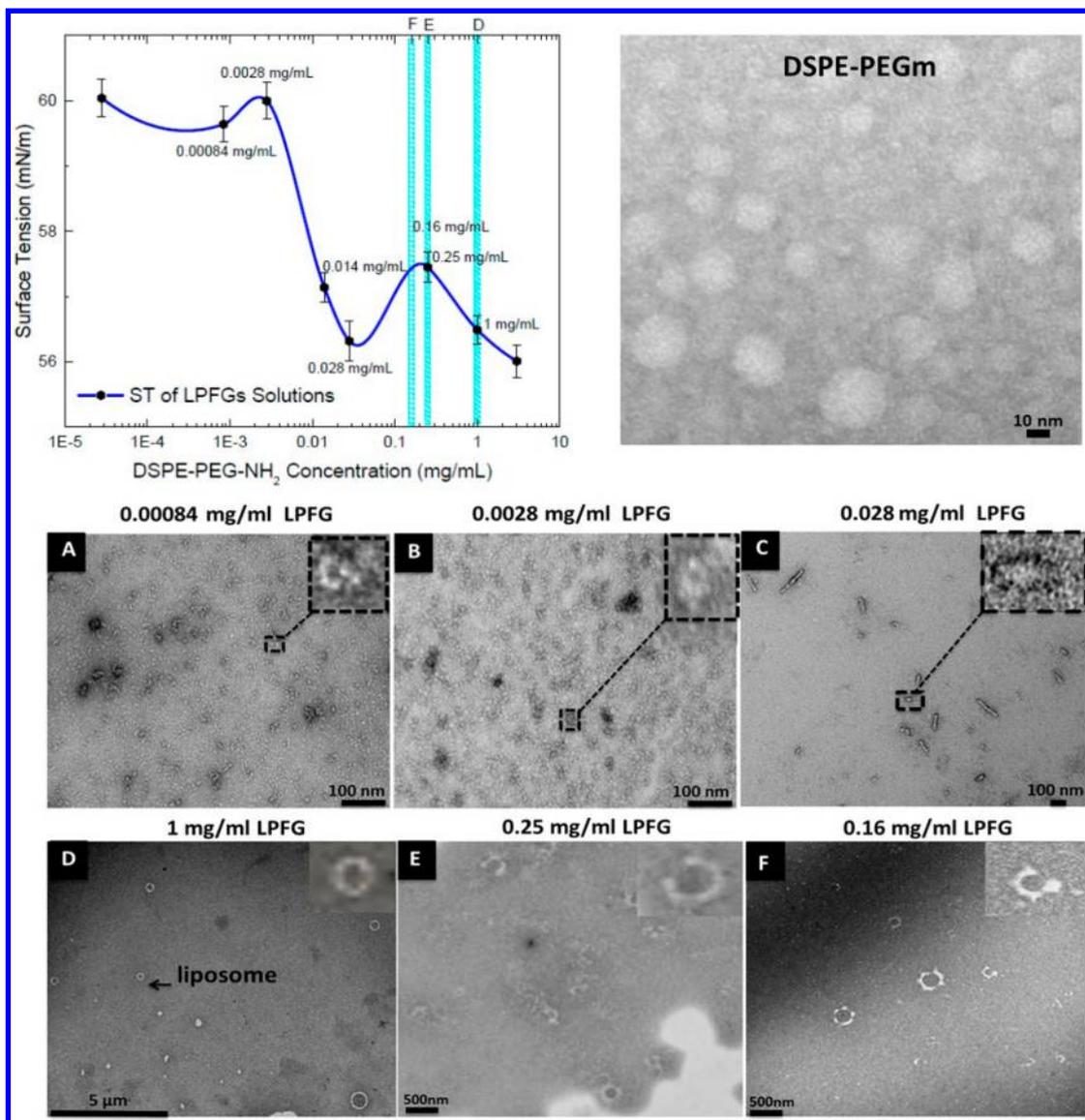
Figure 2. Polymer (1)−polymer (2)−solvent interaction. The graph shows changes in the ST of DSPE-PEG-NH$_2$ while increasing its concentration. For practical purposes, DSPE-PEG-NH$_2$ is named as LPFGs in the figure. The TEM micrograph on the right side of the figure shows the formation of micelles at the CMC of DSPE-PEGm, which occurs at 0.0028 mg/mL. The CMC of DSPE-PEG-NH$_2$ seems to takes place around 0.0028 mg/mL (B). Above this concentration, DSPE-PEG-NH$_2$ tends to form distinctive lipid-based structures. (C) Formation of rod-like shape structures. (D) Formation of well-defined liposomes at the concentration of 1 mg/mL. (E) Disrupted liposomes are observed at 0.25 mg/mL because the incorporation of extra 4% ethanol, which dilutes the LPFGs' concentration (1 mg/mL) and thus affects their physical stability. (F) Further disruptive liposomes are formed at 0.16 mg/mL due to the addition of extra 4% ethanol and PLGA dissolved in ethyl acetate.

shown in Figure 2F. A higher number of fragmented liposomes are observed in the polymer−solvent mixture after adding PLGA previously dissolved in ethyl acetate (Figure 2F). These experimental observations indicate that the solvent−solvent interaction plays a significant role in the polymer−solvent interaction, and therefore it seems that the solvent−solvent interaction drives the phase segregation phenomenon of the polymer blend (i.e., LPFGs and PLGA).

After the pre-emulsification step, the polymer mixture solution is emulsified at 4000 rpm with a high shear mixer. By examining the emulsified solution at different times, we found that the patches are formed quite rapidly within a second time frame. The SEM image in Figure 3A shows the formation of patches after emulsifying the polymer blend for 1 min. Although the patch is already formed after the emulsification step, the patchy particles need to undergo a hardening process
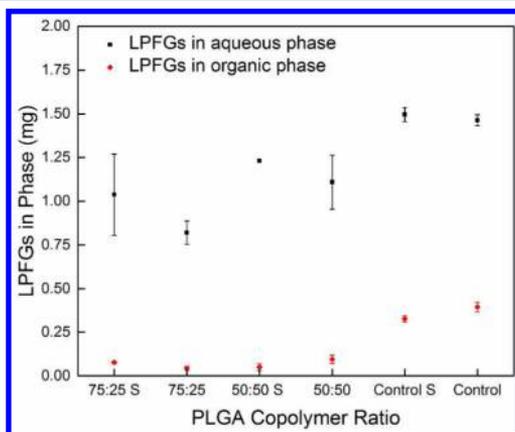
in which the solvent is evaporated, and water is added to the emulsified solution to diffuse the solvent out. After we evaporated and filtered out the solvent using a centrifugal filtration device, patchy particles were obtained. Next, we investigated if the evaporation time is a parameter that has an effect on patch formation. SEM images show that the evaporation time does not have an effect in the formation of patches, as shown in Figure 3B,C. Well-defined patches are formed on the particle's surface after the emulsification step and after 8 and 16 h of solvent evaporation.

Polymer−Polymer−Solvent Interaction. To investigate the polymer (1)−polymer (2)−solvent interaction, we determined the percentage of the reacted LPFGs with PLGA by using an in-house colorimetric method based on fluorescence spectroscopy. Such interaction was determined by comparing samples vigorously shaken manually for 30 s with
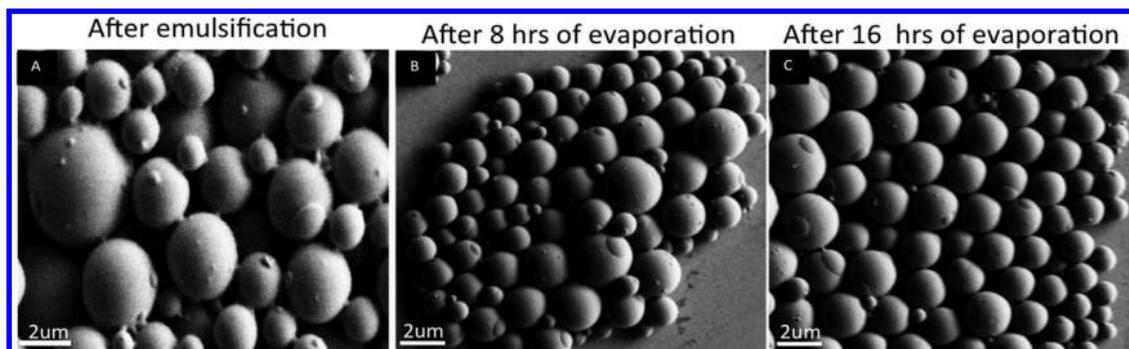
Figure 3. SEM studies after the emulsification, during and after the solvent evaporation step. (A) The SEM image shows the formation of the particle's patch immediately after the emulsification step and before the solvent evaporation step. This means that the formation of the patch takes place during the emulsification step and not in other steps of the particle's synthesis. (B) Patchy particles after 8 h of solvent evaporation. (C) Patchy particles after 16 h of solvent evaporation.

samples in which the polymer blend was emulsified using a high shear mixer, allowing the emulsions to segregate. After the segregation step, the amount of LPFGs in each separated phase was determined by detecting the fluorescence signal of a covalently bound fluorophore. A control experiment containing LPFGs, ethanol, and ethyl acetate without the presence of PLGA was conducted to determine both the LPFGs−solvent interactions and the extent to which PLGA affects the fate of LPFGs during the synthesis. The colorimetric method revealed the way the LPFGs behave without the influence of PLGA. After the phase segregation of the organic and aqueous phases, a considerable amount of LPFGs was found in the aqueous phase as illustrated in Figure 4. The amount of LPFGs in the aqueous phase increases when PLGA is absent (i.e., control experiments). Also, a notably larger amount of LPFGs was detected in the organic phase of the separated emulsion in the

absence of PLGA, contrary to the small amount of LPFGs detected when PLGA is present in the polymer blend.

Polymer−Polymer Interaction When Varying the PLGA Copolymer Ratio. We conducted a series of experiments similar to the ones described above. We observed the same trend with particles synthesized with PLGA of 50:50 copolymer ratio. This result indicates the role PLGA plays in the solubility of LPFGs in the organic solution. This means that PLGA may block or mediate the migration of lipids into that phase upon mixing. In addition, through the colorimetric method we determined the polymer−solvent interaction percentage as shown in Table 1, assuming any undetected

Table 1. Percentage Loss of LPFGs after the Polymer Blend (i.e., PLGA and LPFGs) Was Emulsified

copolymer ratio	inherent viscosity (dL/g)	% of undetected LPFGs in both phases	% of interacted LPFGs with PLGA
75:25	0.55−0.75	43 ± 4.0	57 ± 4.0
50:50	0.55−0.75	60 ± 11	40 ± 11
50:50	0.95−1.20	47 ± 22	53 ± 22
no PLGA		7.2 ± 1.2	

lipids from the amount used in the synthesis are interacting directly with PLGA. This table shows that when particles are synthesized with PLGA (75:25), 57% of the starting weight of LPFGs used for particle synthesis is utilized to form the shell and patch. Second, the extent of miscibility between the polymers seems dependent not only on the shear stress applied to the polymer blend but also on the copolymer ratio. Particles synthesized with PLGA (50:50) influence the extent of miscibility between PLGA and LPFGs. The lower the ratio of lactic acid monomer in the copolymer, the lower the miscibility of the polymers because PLGA with a higher glycolic acid ratio is generally less hydrophobic.[44] Remember the DSPE is the fragment of LPFGs by which the miscibility takes place. Despite the fact that the molecular weight of DSPE is smaller than PLGA, its hydrophobic nature makes the interaction between the PLGA and LPFGs possible.

Polymer−Polymer Interaction When Varying the Copolymer Ratio and Inherent Viscosity of PLGA. To further analyze the role of the copolymer ratio of PLGA in the miscibility with LPFGs, we investigated the effect of the PLGA's inherent viscosity (IV) on such miscibility. To achieve this task, we determined the interaction of PLGA (50:50) and LPFGs by varying the IV of the copolymer. The inherent

Figure 4. Quantification of LPFGs in the aqueous and organic phases after phase segregation. Black squares represent LPFGs present in the aqueous phase of the emulsion, and red diamonds represent LPFGs present in the organic phase of the separated emulsion. S indicates samples that were manually shaken rather than being homogenized. 50:50 PLGA has a similar degree of polymerization to 75:25 PLGA. Control samples contained no PLGA. In the polymer blend that is emulsified at 4000 rpm less LPFGs were detected in the organic phase, which suggests that LPFGs have interacted with PLGA to form shells and patches. The presence of PLGA in the organic phase limits the solubility of LPFGs, as indicated by the higher LPFGs concentration in the organic phase of the control samples than the ones determined in the test samples.

viscosity is related to the number-average molecular weight (M_n) of the polymer; thus, a higher IV indicates a longer chain length.[45] The chain length is related to the free energy of mixing for the system: each monomer occupies a certain volume, which affects the miscibility of the PLGA and LPFGs. Hence, we hypothesized that changing the PLGA chain length would affect the mobility of PLGA chains based on the lattice model proposed by Flory−Huggins.[46] Longer-chain molecules would occupy more lattice positions, thereby excluding other molecules. However, our experimental results do not fit within the simplified parameters of Flory−Huggins theory and show that the intrinsic viscosity played a negligible role in the miscibility between PLGA and LPFGs as shown in Figure 5.
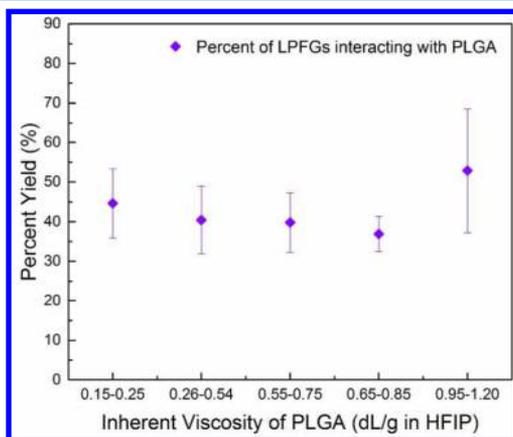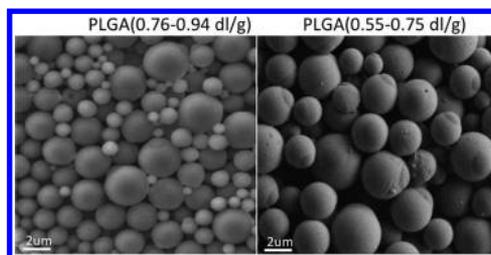

Figure 5. Effect of the inherent viscosity in the miscibility of PLGA and LPFGs. Taking into consideration the standard error of the data, there is not a correlation between the inherent viscosity and LPFGs-PLGA interactions, which suggests that the monomer volume fractions do not play a major role in the degree of miscibility between these polymers.

Each of the PLGA samples with different IV exhibited similar ranges of percent yield of lipids to PLGA, revealing that the IV and molecular weight of PLGA do not heavily influence patch formation. 50:50 PLGA with an IV of 0.95−1.20 dL/g in hexafluoroisopropanol (HFIP), based on stoichiometric calculations, has the most similar degree of polymerization to the 75:25 PLGA of the selected viscosities (0.55−0.75 dL/g). The higher ratio of lactic acid in our 75:25 copolymer system allows for unique miscibility between the DSPE-PEG-NH$_2$ and the PLGA. Nevertheless, the solvent−solvent interaction seems to drive the phase segregation phenomenon of the polymer blend.

In addition, we synthesized particles with PLGA of different inherent viscosities 0.55−0.75 and 0.76−0.94 dL/g to investigate if the molecular weight of PLGA has an effect in the formation of patchy particles. As it is known, the molecular weight of the polymer can be obtained based on the inherent viscosity of the polymer. We found that the molecular weight of PLGA and therefore the inherent viscosity do not have a role in the formation of patchy particles. Figure 6 shows that well-defined patches are formed at two different inherent viscosities.

Role of Solvent Composition in Polymer Behavior. To study in depth the role of the solvent composition in polymer's behavior, we conducted a series of experiments where we varied the solvent composition. The SEM micrographs in Figure 7A confirm that the solvent composition has a strong influence on the behavior of the LPFGs. This behavior might determine the particles' final morphology. Particles with a patch−core−shell


Figure 6. Effect of the inherent viscosity and molecular weight of PLGA in the formation of patchy particles. Patchy particles were synthesized with two different inherent viscosities 0.55−0.75 and 0.76−0.94 dL/g. It was found that these factors do not have an effect in the formation of patchy particles because there is no difference in the morphology of the particles.

structure are formed when the ethanol is present at 3 wt %. Particles synthesized at different volume percentages of ethanol were analyzed using a differential scanning calorimeter (DSC). These samples exhibited similar enthalpies of transition to other particles studied (Figure 7B). Interestingly, there was no direct correlation between the percentage of ethanol used in the synthesis and the magnitude of the enthalpy of transition. An increase in ethanol composition does not predictably affect the particles' thermodynamics. This result suggests that a more complex phenomenon is driving the different patch morphologies shown in Figure 7A.

Interfacial Surface Tension (IST). Examining further the role of ethanol in the formation of patches, we measured the interfacial surface tension (IST) of the polymer−lipid−polymer−solvent mixture while varying the volume percentage of ethanol in the presence and absence of LPFGs. We found that as the volume percent of ethanol increases in the aqueous phase, the IST between the organic and aqueous phases of the solvent system decreases. This trend is observed in the absence and presence of LPFGs, as illustrated in Figure 8. Ethanol in particular influences the lipids' behavior. For example, particles synthesized in the absence of ethanol display formation of multiple and randomly distributed lipid-based nanostructures on the particle's core, as shown in Figure 7A.

Role of the Shear Stress in the Formation of Patchy Particles. After the solvent−solvent and polymer−polymer−solvent analyses, we reached the conclusion that the formation of patchy particles was strongly dependent on a physical parameter such as the shear stress. We studied this parameter in detail during the emulsification step. During this step, the aqueous and organic phases are emulsified with a high shear mixer; thus, the polymer blend solution undergoes a shear stress. We found that the shear stress was indeed a physical parameter that is critical for the formation of patchy particles. This statement is based on the fact that the shear stress promotes and enhances the mutual miscibility between PLGA and LPFGs (Figure 9B−D). Particles with a core−shell structure are formed when the polymer blend solution undergoes low shear stress (Figure 9A). On the contrary, particles with a core−shell−patch structure are only formed when the polymer blend undergoes high shear stress during emulsification step (Figure 9C). Furthermore, we observed that when the shear stress is low, LPFGs form a very thin shell on the polymeric core as observed in the cross section of the core−shell particles (Figure 9B) and as shown by the differential scanning calorimetry (DSC) thermograms (Figure 9E).
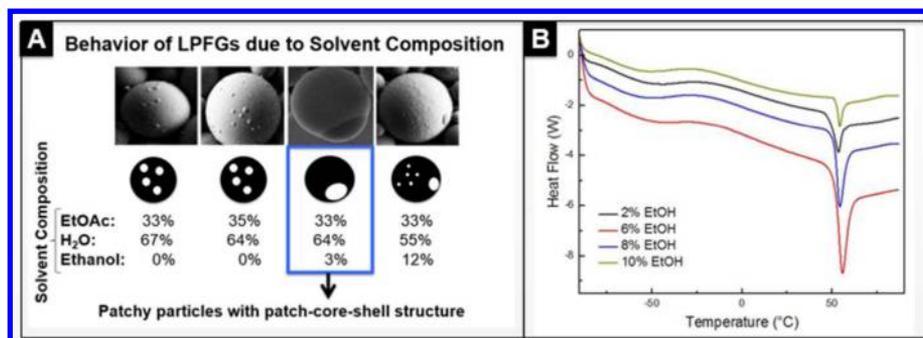
Figure 7. Effect of the solvent composition in particle's morphology. (A) The solvent composition strongly influences the LPFGs' behavior. (B) DSC thermograms of particles synthesized with different volume percentage of ethanol. The solvent composition has a strong effect on the phase transition behavior of LPFGs. However, increments in ethanol do not have a direct linear correlation with the enthalpy of the system over the range of temperatures. The absence of ethanol in the solvent mixture induces the formation of lipid-based nanostructures on the polymeric cores (Figure 6A,B). Particles with a patch−shell−core structure are formed when the percentage of ethanol is 3%. Particles synthesized with 12% ethanol and above display lipid-based nanostructures on the particles' surfaces as shown by the SEM micrographs (Figure 6A).
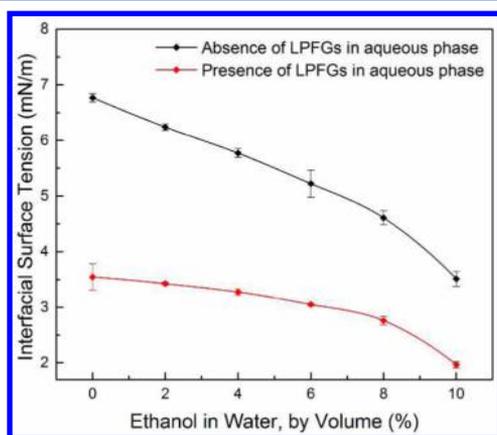

Figure 8. Effect of ethanol in the interfacial surface tension of PLGA in the presence and absence of LPFGs. Red diamonds indicate samples containing 0.25 mg/mL of LPFGs in the aqueous phase, while black diamonds indicate samples containing only the stated ethanol percentage dissolved in water. As the volume percentage of ethanol increases in the solvent mixture, the IST between the organic and aqueous phases decreases. The decrement of the interfacial surface tension in the solvent mixture has a strong influence on the behavior of the LPFGs. Lipid-based nanostructures are formed in the absence of ethanol whereas a patch−shell−core structure is formed when 3% ethanol is present in the solvent mixture.

The partial miscibility of the polymers gives rise to the formation of the particle's shell. The DSPE fragment of LPFGs interacts with PLGA via hydrophobic interactions, which makes possible the formation of the particle's shell. The shell indicates the extent of the phase segregation phenomenon between these two polymers with a certain degree of miscibility, allowing for two distinct but adhered phases. Also, polymers undergo phase transitions at characteristic temperatures, including melting temperatures for crystalline polymers (T_m) and glass transition temperatures (T_g) for amorphous materials.[47] Miscible polymers exhibit phase transition temperatures in between the phase transitions of the component polymers in the mixture. The phase transition temperature can be used to distinguish miscible and immiscible materials.[45,48] In our studies, PLGA had a glass transition temperature of 56.48 °C, while the LPFGs had a melting point of 54. 48 °C (Figure 9E). A mixture of PLGA and LPFGs would exhibit a phase transition endotherm that shares the characteristics of the component

polymers, whereas the phase-segregated patch would exhibit both phase transitions separately. Thermograms of both the core−shell particles and the patch−shell−core particles were recorded. Core−shell particles have a phase transition at 55.44 °C, and patchy particles have a phase transition at 55.32 °C. These numbers do suggest a certain degree of miscibility, although these temperatures are very close. What is more interesting is the enthalpy of transition, which is the integral of the phase transition endotherm.[49] LPFGs have a large enthalpy of transition in the characteristic shape of a T_m, while PLGA has a relatively shallow phase transition. Referring to the shape and integration of the particle endotherms, we can see a clear difference between the core−shell particles and the patchy particles, as shown in Figure 9E, inset. The core−shell particles' thermogram very closely matches with the PLGA endotherm, with a similar enthalpy of transition. Patchy particles, on the other hand, exhibit a glass transition endotherm that has a higher change in enthalpy than the PLGA. The glass transition shape, coupled with the larger change in enthalpy, suggests unique phase transitions occurring between the phase-separated patch and particle, which are only miscible to a slight degree.

The magnitude of the shear stress is determined by the distance between the homogenizer's workheads and the rotor shaft. The smaller the gap, the higher the shear stress that the polymer solution undergoes during the particle's synthesis, as observed experimentally and corroborated with computational fluid dynamics (CFD) simulations (Figure 10A−G) (see Supporting Information to play the movie of this CFD). These experimental and computational results show that when the gap between the inner diameter of the workhead and the rotor-shaft is greater than 0.137 mm in each side of the rotor-shaft, only particles with a core−shell structure are formed (Figure 9A,B). Patchy particles are formed in the presence of high shear stress, which is generated with a gap size below 0.1 mm (Figure 9C,D). The shear stress determines not only the morphology of the particle (i.e., core−shell−patch and core−shell) but also the thickness of the shell (Figure 9B−D). The higher the shear stress, the thicker the particle's shell, as shown by the cross sections of these particles (Figure 9D). Thus, the shear stress is the most important parameter for the formation of patchy particles. Further studies on CFD will be useful to further understand the formation of patchy particles and to tune the external and internal properties of these polymeric particles.
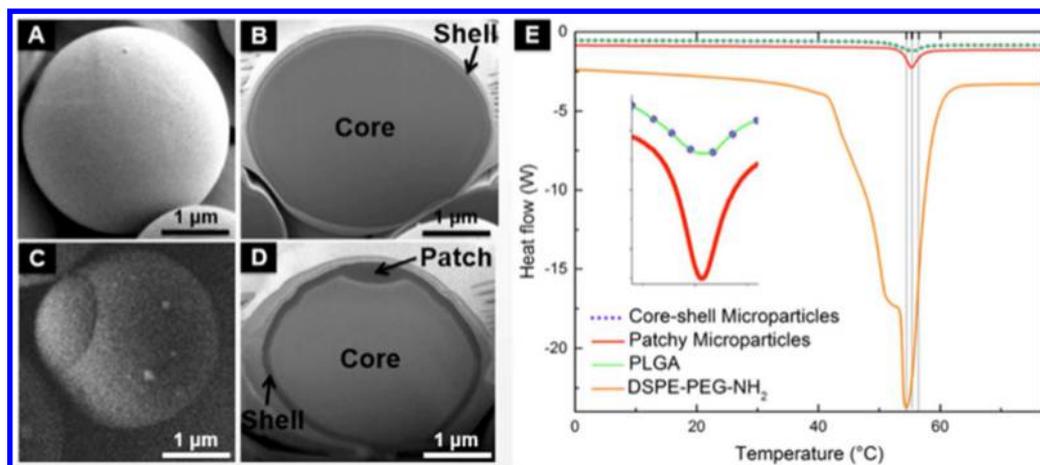
Figure 9. Effect of the shear stress in particle's morphology. (A) SEM image and (B) FIB cross-section of a particle with a core-shell structure under low shear stress. (C) SEM image and (D) FIB cross-section of a particle with a patch–shell–core structure under high shear stress. (E) Differential scanning calorimetry (DSC) thermograms: (black) thermogram derived from particles that have a core–shell structure; (blue) thermogram derived from particles with a patch–shell–core structure; (red) thermogram of PLGA. All of these particles have the same glass transition temperature. High shear stress enhances the miscibility between PLGA and LPFGs. As a result, a thick shell is formed in patchy particles.
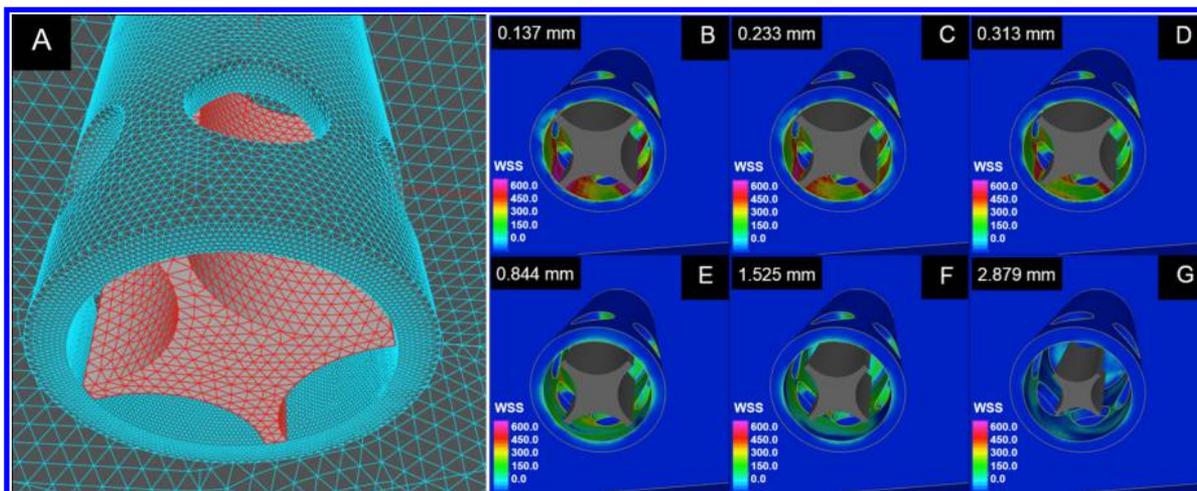

Figure 10. Computational fluid dynamics (CFD) on the wall shear stress. (A) 3D model of the homogenizer tubular assembly 5/8 in. workhead (blue) and rotor-shaft (red). (B–G) Wall shear stress at different gap sizes. As the gap between the internal diameter of the homogenizer's workhead and the rotor shaft decreases, the wall shear stress increases and occurs in larger region of the blades. Patchy particles are formed when the gap size in each side is below 0.1 mm.

On the basis of the results obtained through the study of the chemical (solvent–solvent, polymer–solvent, polymer–polymer–solvent interaction) and physical (shear stress) factors that are involved in the synthesis of patchy polymeric particles, we suggest the following mechanism for the formation of patchy polymeric particles. During the pre-emulsification step, the LPFGs form liposomes (e.g., multilamellar and unilamellar vesicles) because the concentration of LPFGs used in the particle's synthesis is above the critical micelle concentration (CMC) of DSPE-PEGm (1a) (i.e ∼0.0028 mg/mL). However, because of the incorporation of extra ethanol, ethyl acetate and PLGA, the physical integrity of these liposomes is affected (1b). When previously dissolved PLGA in ethyl acetate is incorporated into the aqueous phase, a phase segregation phenomenon takes places initiated by the solvents (i.e., water–ethanol and ethyl acetate). The DSPE fragment of LPFGs interacts favorably and rapidly with the PLGA during the pre-emulsification step. The polymer blend undergoes a high shear stress during the emulsification step, which promotes the miscibility between PLGA and LPFGs giving rise to a droplet with a core–shell structure (2a). The presence of high shear stress enhances the miscibility of the polymer blend inducing a pronounced phase segregation phenomenon that results in the formation of the core–shell structure followed by the formation of the patch. That is, during these chemical and physical conditions, droplets coated with LPFGs having an indentation are formed, and the remaining LPFGs start forming the patch (2b). The patch may be formed by a pile-up of lipid-based structures (2c). The patchy particles that result from this process have a hollow core, as shown by the cross sections of these particles (see Supporting Information), a shell formed by PLGA-DSPE-PEG-NH$_2$, and a patch formed by a pile-up of LPFGs. The entire mechanism of the formation of patchy particles is summarized in Figure 11.

4. CONCLUSIONS

In summary, we have elucidated the mechanisms involved in the formation of patchy polymeric particles by analyzing each
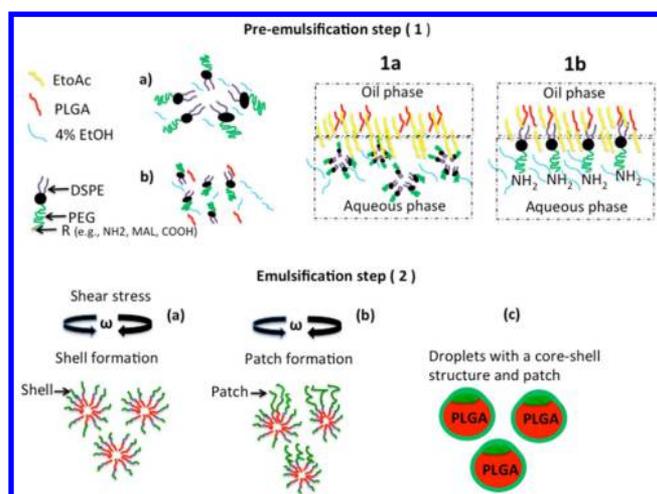
Figure 11. Mechanisms of the formation of patchy polymeric hollow particles. In the pre-emulsification step, the solvent system (H₂O, EtOH, and EtOAc) and polymers (LPFGs and PLGA) interact with each other (1a,b). In the emulsification step, patchy particles are formed in the presence of high shear stress conditions. The particle's core−shell structure is formed (2a) followed by the formation of the patch (2b). The patch is likely to be formed by a pile-up of LPFGs (2c).

step in their synthesis. We found that the shear stress is the most important parameter that causes the formation of lipid−polymeric patchy particles. Also, the interplay of solvent−solvent, polymer−solvent, and polymer−polymer−solvent composition and shear stress render particles with lipid-based structures on their surfaces. These key results allow us to have a much better understanding of the formation of hollow polymeric patchy particles and therefore to acquire high control of the physicochemical properties of these particles. Because today LPFGs have been extensively used in engineering drug delivery systems (DDS),[50−52] the results reported in this article allow us to understand their unexpected behavior under different shear stress conditions. In addition, this paper contributes to the particles field by revealing that the shear stress is a physical parameter that can be useful to synthesize particles with different external and internal morphologies and thermal properties, as shown by DSC thermograms. By understanding the formation of patchy particles, we can control their internal and external physicochemical properties, which can potentially revolutionize medicine and fields including electronics, energy, and environmental chemistry, among others. Future research at the experimental and computational level is needed to further understand the role of shear stress in the formation of patchy particles and to elucidate the arrangement of the LPFGs in the particle's patch.

ASSOCIATED CONTENT

ⓈSupporting Information

Movies of cross sections of patchy particles and computational fluid dynamics simulations. The Supporting Information is available free of charge on the ACS Publications website at DOI: 10.1021/acs.langmuir.5b01551.

AUTHOR INFORMATION

Corresponding Author
*E-mail: csalvado@gmu.edu (C.S.-M.).

REFERENCES
(1) Glotzer, S. C.; Solomon, M. J. Anisotropy of Building Blocks and Their Assembly into Complex Structures. *Nat. Mater.* **2007**, *6*, 557−562.
(2) Millan, J. A.; Ortiz, D.; van Anders, G.; Glotzer, S. C. Self-Assembly of Archimedean Tilings with Enthalpically and Entropically Patchy Polygons. *ACS Nano* **2014**, *8*, 2918−2928.
(3) Rovigatti, L.; de las Heras, D.; Tavares, J. M.; Telo da Gama, M. M.; Sciortino, F. Computing the Phase Diagram of Binary Mixtures: a Patchy Particle Case Study. *J. Chem. Phys.* **2013**, *138*, 164904−164915.
(4) Van Anders, G.; Ahmed, N. K.; Smith, R.; Engel, M.; Glotzer, S. C. Entropically Patchy Particles: Engineering Valence Through Shape Entropy. *ACS Nano* **2014**, *8*, 931−940.
(5) Shah, A. A.; Schultz, B.; Kohlstedt, K. L.; Glotzer, S. C.; Solomon, M. J. Synthesis, Assembly, and Image Analysis of Spheroidal Patchy Particles. *Langmuir* **2013**, *29*, 4688−4696.
(6) Pons-Siepermann, I. C.; Glotzer, S. C. Design of Patchy Particles Using Ternary Self-Assembled Monolayers. *Soft Matter* **2012**, *8*, 6226−6231.
(7) Santos, A.; Millan, J. A.; Glotzer, S. C. Facetted Patchy Particles through Entropy-Driven Patterning of Mixed Ligand SAMS. *Nanoscale* **2012**, *4*, 2640−2650.
(8) Rezvantalab, H.; Shojaei-Zadeh, S. Designing Patchy Particles for Optimum Interfacial Activity. *Phys. Chem. Chem. Phys.* **2014**, *16*, 8283−8293.
(9) Preisler, Z.; Vissers, T.; Munao, G.; Smallenburg, F.; Sciortino, F. Equilibrium Phases of One-Patch Colloids with Short-Range Attractions. *Soft Matter* **2014**, *10*, 5121−5128.
(10) Bao, H.; Bihr, T.; Smith, A. S.; Klupp Taylor, R. N. Facile Colloidal Coating of Polystyrene Nanospheres with Tunable Gold Dendritic Patches. *Nanoscale* **2014**, *6*, 3954−3966.
(11) Wang, Y.; Wang, Y.; Zheng, X.; Yi, G. R.; Sacanna, S.; Pine, D. J.; Weck, M. Three-Dimensional Lock and Key Colloids. *J. Am. Chem. Soc.* **2014**, *136*, 6866−6869.
(12) Mehringer, C.; Wagner, R.; Jakuttis, T.; Butz, B.; Spiecker, E.; Peukert, W. Gas Phase Synthesis of Anisotropic Silicon Germanium Hybrid Nanoparticles. *J. Aerosol Sci.* **2014**, *67*, 119−130.
(13) Higuchi, T.; Tajima, A.; Motoyoshi, K.; Yabu, H.; Shimomura, M. Frustrated Phases of Block Copolymers in Nanoparticles. *Angew. Chem.* **2008**, *47*, 8044−8046.
(14) Zhang, G.; Wang, D.; Mohwald, H. Patterning Microsphere Surfaces by Templating Colloidal Crystals. *Nano Lett.* **2005**, *5*, 143−146.
(15) Cui, J. Q.; Kretzschmar, I. Surface-Anisotropic Polystyrene Spheres by Electroless Deposition. *Langmuir* **2006**, *22*, 8281−8284.
(16) Rozynek, Z.; Mikkelsen, A.; Dommersnes, P.; Fossum, J. O. Electroformation of Janus and Patchy Capsules. *Nat. Commun.* **2014**, *5*, 1−6.
(17) Pawar, A. B.; Kretzschmar, I. Fabrication, Assembly, and Application of Patchy Particles. *Macromol. Rapid Commun.* **2010**, *31*, 150−168.

(18) Perro, A.; Reculusa, S.; Ravaine, S.; Bourgeat-Lami, E. B.; Duguet, E. Design and synthesis of Janus Micro- and Nanoparticles. *J. Mater. Chem.* **2005**, *15*, 3745−3760.

(19) Roh, K. H.; Martin, D. C.; Lahann, J. Biphasic Janus Particles with Nanoscale Anisotropy. *Nat. Mater.* **2005**, *4*, 759−763.

(20) Roh, K. H.; Martin, D. C.; Lahann, J. Triphasic Nanocolloids. *J. Am. Chem. Soc.* **2006**, *128*, 6796−6797.

(21) Lim, D. W.; Hwang, S.; Uzun, O.; Stellacci, F.; Lahann, J. Compartmentalization of Gold Nanocrystals in Polymer Micro-particles Using Electrohydrodynamic Co-Jetting. *Macromol. Rapid Commun.* **2010**, *31*, 176−182.

(22) Bhaskar, S.; Gibson, C. T.; Yoshida, M.; Nandivada, H.; Deng, X.; Voelcker, N. H.; Lahann, J. Engineering, Characterization and Directional Self-Assembly of Anisotropically Modified Nanocolloids. *Small* **2011**, *7*, 812−819.

(23) Ding, T.; Smoukov, S. K.; Baumberg, J. J. Harnessing Nonlinear Rubber Swelling for Bulk Synthesis of Anisotropic Hybrid Nano-particles. *J. Mater. Chem. C* **2014**, *2*, 8745−8749.

(24) Hong, L.; Jiang, S.; Granick, S. Simple Method to Produce Janus Colloidal Particles in Large Quantity. *Langmuir* **2006**, *22*, 9495−9499.

(25) Manoharan, V. N.; Elsesser, M. T.; Pine, D. J. Dense Packing and Symmetry in Small Clusters of Microspheres. *Science* **2003**, *301*, 483−487.

(26) Cho, Y. S.; Yi, G. R.; Lim, J. M.; Kim, S. H.; Manoharan, V. N.; Pine, D. J.; Yang, S. M. Self-Organization of Bidisperse Colloids in Water Droplets. *J. Am. Chem. Soc.* **2005**, *127*, 15968−15975.

(27) Yake, A. M.; Snyder, C. E.; Velegol, D. Site-Specific Functionalization on Individual Colloids: Size Control, Stability, and Multilayers. *Langmuir* **2007**, *23*, 9069−9075.

(28) Snyder, C. E.; Yake, A. M.; Feick, J. D.; Velegol, D. Nanoscale Functionalization and Site-Specific Assembly of Colloids by Particle Lithography. *Langmuir* **2005**, *21*, 4813−4815.

(29) Pawar, A. B.; Kretzschmar, I. Patchy Particles by Glancing Angle Deposition. *Langmuir* **2008**, *24*, 355−358.

(30) Pawar, A. B.; Kretzschmar, I. Multifunctional Patchy Particles by Glancing Angle Deposition. *Langmuir* **2009**, *25*, 9057−9063.

(31) Salvador-Morales, C.; Valencia, P. M.; Gao, W.; Karnik, R.; Farokhzad, O. C. Spontaneous Formation of Heterogeneous Patches on Polymer-Lipid Core-Shell Particle Surfaces during Self-Assembly. *Small* **2013**, *9*, 511−517.

(32) Romanski, F. S.; Winkler, J. S.; Riccobene, R. C.; Tomassone, M. S. Production and Characterization of Anisotropic Particles from Biodegradable Materials. *Langmuir* **2012**, *28*, 3756−3765.

(33) Kim, M. R.; Lee, S.; Park, J. K.; Cho, K. Y. Golf Ball-Shaped PLGA Microparticles with Internal Pores Fabricated by Simple O/W Emulsion. *Chem. Commun.* **2010**, *46*, 7433−7435.

(34) Nishi, T.; Wang, T. T.; Kwei, T. K. Thermally Induced Phase Separation Behavior of Compatible Polymer Mixtures. *Macromolecules* **1975**, *8*, 227−234.

(35) Kietzke, T.; Neher, D.; Kumke, M.; Ghazy, O.; Ziener, U.; Landfester, K. Phase Separation of Binary Blends in Polymer Nanoparticles. *Small* **2007**, *3*, 1041−1048.

(36) Narasimhan, V.; Lloyd, D. R.; Burns, C. M. Phase Equilibria of Polystyrene-Polybutadiene-Tetrahydrofuran Using Gel-Permeation Chromatography. *J. Appl. Polym. Sci.* **1979**, *23*, 749−754.

(37) Habersberger, B. M.; Bates, F. S.; Lodge, T. P. Hierarchical Microphase Separation in Bicontinuous Ternary Polymer Blends. *Soft Matter* **2012**, *8*, 3429−3441.

(38) Ellison, C. J.; Meuler, A. J.; Qin, J.; Evans, C. M.; Wolf, L. M.; Bates, F. S. Bicontinuous Polymeric Microemulsions from Poly-disperse Diblock Copolymers. *J. Phys. Chem. B* **2009**, *113*, 3726−3737.

(39) Lee, H. S.; Kim, W. N.; Burns, C. M. Determination of the Flory-Huggins Interaction Parameter of Polystyrene-Polybutadiene Blends by Thermal Analysis. *J. Appl. Polym. Sci.* **1997**, *64*, 1301−1308.

(40) Lingwood, D.; Simons, K. Lipid Rafts as a Membrane-Organizing Principle. *Science* **2010**, *327*, 46−50.

(41) Resa, J. M.; Goenaga, J. M.; Iglesias, M.; Gonzalez-Olmos, R.; Pozuelo, D. Liquid-liquid Equilibrium Diagrams of Ethanol + Water +

(Ethyl Acetate or 1-Pentanol) at Several Temperatures. *J. Chem. Eng. Data* **2006**, *51*, 1300−1305.

(42) Hansen, C. M. Solubility Parameters-An Introduction. In *Hansen Solubility Parameters: A User's Handbook*; CRC Press: Boca Raton, FL, 2000; pp 1−24.

(43) Kastantin, M.; Ananthanarayanan, B.; Karmali, P.; Ruoslahti, E.; Tirrell, M. Effect of the Lipid Chain Melting Transition on the Stability of DSPE-PEG (2000) Micelles. *Langmuir* **2009**, *25*, 7279−7286.

(44) Edlund, U.; Albertsson, A. C. Degradable Polymer Microspheres for Controlled Drug Delivery. *Adv. Polym. Sci.* **2002**, *157*, 67−112.

(45) Rodriguez, F.; Cohen, C.; Ober, C. K.; Archer, L. A. *Principles of Polymer Systems*, 5th ed.; Taylor and Francis: New York, 2003.

(46) Sariban, A.; Binder, K. Critical Properties of the Flory-Huggins Lattice Model of Polymer Mixtures. *J. Chem. Phys.* **1987**, *86*, 5859−5873.

(47) Ebewele, R. O. Thermal Transitions in Polymers. *Polymer Science and Technology*; CRC Press: Boca Raton, FL, 2000; pp 95−116.

(48) Xiao, C. D.; Shen, X. C.; Tao, L. Modified Emulsion Solvent Evaporation Method for Fabricating Core-Shell Microspheres. *Int. J. Pharm.* **2013**, *452*, 227−232.

(49) Willson, R. J. Calorimetry. In *Principles of Thermal Analysis and Calorimetry*; Haines, P. J., Ed.; Royal Society of Chemistry: Cambridge, UK, 2002; pp 129−165.

(50) Liechty, W. B.; Kryscio, D. R.; Slaughter, B. V.; Peppas, N. A. Polymers for Drug Delivery Systems. *Annu. Rev. Chem. Biomol. Eng.* **2010**, *1*, 149−173.

(51) Elvira, C.; Gallardo, A.; Roman, J. S.; Cifuentes, A. Covalent Polymer-Drug Conjugates. *Molecules* **2005**, *10*, 114−125.

(52) Emeje, M. O.; Obidike, I. C.; Akpabio, E. I.; Ofoefule, S. I. Nanotechnology in Drug Delivery. In *Recent Advances in Novel Drug Carrier Systems*; Sezer, A. D., Ed.; InTech: Rijeka, Croatia, 2012; pp 69−106.